9. Morgan KG, Bryant SH. The mechanism of action of dantrolene sodium. *J Pharmacol Exp Ther* 1977;201:138–147.
10. Sutko JL, Kenyon JL. Ryanodine modification of cardiac muscle responses to potassium-free solutions. Evidence for inhibition of sarcoplasmic reticulum calcium release. *J Gen Physiol* 1983;82:385–404.
11. Taylor A, Nally J, Aurell M, et al. Consensus report on ACE inhibitor renography for detecting renovascular hypertension. *J Nucl Med* 1996;37:1876–1882.
12. Roccatello D, Picciotto G, Rabbia C, et al. Prospective study on captopril renography in hypertensive patients. *Am J Nephrol* 1992;12:406–411.
13. Patrois F, Hignette C, Froissart M, Prigent A. Captopril renal scintigraphy interpretation: a bilateral false-positive case. *Médecine nucléaire* 1995;13:309–313.
14. Fleming JT, Parekh N, Steinhausen M. Calcium antagonists preferentially dilate preglomerular vessels of hydronephrotic kidney. *Am J Physiol* 1987;253(6 pt2): F1157–F1163.

Comparative Study of Technetium-99m-Sestamibi and Thallium-201 SPECT in Predicting Chemotherapeutic Response in Small Cell Lung Cancer

Yuka Yamamoto, Yoshihiro Nishiyama, Katashi Satoh, Hitoshi Takashima, Motoomi Ohkawa, Jiro Fujita, Toshiyuki Kishi, Shinsuke Matsuno and Masatada Tanabe

Department of Radiology and First Department of Internal Medicine, Kagawa Medical University, Kagawa; and Departments of Radiology and Internal Medicine, Takinomiya General Hospital, Kagawa, Japan

The purpose of this study was to evaluate the relationship between ^{99m}Tc-sestamibi (MIBI) accumulation by tumor and response to chemotherapy in small cell lung cancer patients compared with ^{201}Tl-chloride. **Methods:** There were 19 patients with small cell lung cancer just before chemotherapy initiation. The patients were classified by a follow-up CT into complete remission, partial remission and no change groups. All patients underwent dual-isotope imaging with ^{201}Tl-chloride and ^{99m}Tc-MIBI. Regions of interest were placed over the tumors and contralateral normal lung tissue on one coronal view with a clearly defined lesion, and the tumor-to-normal (T/N) ratio and retention index were calculated. **Results:** Early and delayed T/N ratios for ^{99m}Tc-MIBI in complete remission and partial remission groups were significantly higher ($p < 0.05$) than in the no change group. There was no significant correlation between T/N ratio and tumor response using ^{201}Tl-chloride. There were no significant differences in the retention index with respect to the tumor response in both ^{201}Tl-chloride and ^{99m}Tc-MIBI SPECT images. **Conclusion:** Technetium-99m-MIBI SPECT may be more effective than ^{201}Tl-chloride SPECT for evaluating response to chemotherapy in patients with small cell lung cancer.

Key Words: technetium-99m-sestamibi; thallium-201-chloride; small cell lung cancer; dual-isotope imaging; chemotherapy

J Nucl Med 1998; 39:1626–1629

Use of ^{201}Tl-chloride SPECT is now attracting attention for detection of lung cancer (*1,2*). In recent years, however, several ^{99m}Tc-labeled imaging agents have also been under investigation. Labeling with ^{99m}Tc has several advantages over using ^{201}Tl. Noncardiac uses of ^{99m}Tc-sestamibi (MIBI; hexakis 2-methoxyisobutylisonitrile), such as visualization of lung cancer, have also been investigated. Morphologic imaging techniques such as CT, ultrasonography and MRI cause problems in the evaluation of treatment response and in establishing whether a residual mass is due to a residual tumor or local recurrence. Nuclear medicine imaging techniques may be applicable to the evaluation of therapeutic efficacy and the prediction of therapeutic response in cancer. The primary therapeutic modality for small cell lung cancer is chemotherapy. Resistance of malignant tumors to chemotherapeutic agents is a major cause of treatment failure. In this study, we evaluated the prediction of chemotherapeutic effect using ^{99m}Tc-MIBI SPECT in small cell lung cancer patients in comparison with ^{201}Tl-chloride SPECT.

Received Aug. 6, 1997; revision accepted Dec. 24, 1997.
For correspondence or reprints contact: Yuka Yamamoto, MD, Department of Radiology, Kagawa Medical University, 1750-1 Ikenobe, Miki-cho, Kita-gun, Kagawa 761-07, Japan.

MATERIALS AND METHODS

Patients

There were 19 patients (15 men, 4 women; age range 39–86 yr) with small cell lung cancer who were investigated before chemotherapy. Diagnosis was made by cytologic or histopathologic analysis of sputum, CT-guided needle biopsy or endoscopic samples. The lung lesions were staged according to the tumor-node-metastasis classification. The smallest tumor was 3 cm, and the largest was 8 cm by CT scan. All patients underwent simultaneous dual-isotope SPECT of the chest with ^{201}Tl-chloride and ^{99m}Tc-MIBI just before chemotherapy initiation. After the imaging study, all patients received multidrug chemotherapy regimens consisting of cyclophosphamide, doxorubicin, vincristine, etoposide, cisplatin, mitomycin-C and vindesine. The patients were classified by a follow-up CT examination within 4 wk after last chemotherapy into the following groups: complete remission (CR), when there was no evidence of disease; partial remission (PR), when there was ≥50% decrease in the sum of the product of the maximum perpendicular diameters of all measurable lesions; and no change (NC), when there was <50% decrease in the sum of the product of the maximum perpendicular diameters of all measurable lesions.

Simultaneous Dual-Isotope Imaging

Dual-isotope imaging was performed with a large field-of-view gamma camera, with high resolution and a parallel-hole collimator (Picker Prism 2000; Picker International, Cleveland, OH). This camera was interfaced to a dedicated computer (ODYSSEY; Picker International). Doses of 111 MBq ^{201}Tl-chloride and 600 MBq ^{99m}Tc-MIBI were injected intravenously. Early SPECT acquisition was performed 15 min after the injection of each radioisotope, whereas delayed SPECT images were acquired 2 hr after injection. For SPECT images of chest, 72 projections were obtained using a 64 × 64 matrix for 45 sec/view in a step-and-shoot mode. Using a

dual-head camera, the total actual acquisition time was 27 min. Three energy analyzers were used for acquisition, which were set at 71 keV with a 15% window for ^{201}Tl images, 90 keV with a 10% window for scatter images and 140 keV with a 15% window for ^{99m}Tc images. These projection data were processed with a two-dimensional low-pass filter and then corrected for the contamination scatter. Image reconstruction was performed using filtered backprojection with a ramp filter. Transverse, coronal and sagittal sections were reconstructed. The system was 7 mm FWHM, and the slice thickness was 10 mm. Attenuation correction was not performed.

Contamination Scatter Correction for Each Radionuclide

Because this study involved simultaneous dual-isotope imaging, the raw data at the 71-keV window were contaminated by ^{99m}Tc Compton scatter and the raw data at the 140-keV window included a 167-keV gamma-ray count for ^{201}Tl. Therefore, the raw ^{201}Tl and ^{99m}Tc data were corrected to eliminate such contamination scatter, according to the equations in each pixel. Simultaneously acquired dual-isotope ^{201}Tl/^{99m}Tc SPECT studies were performed using the original shape and size of the phantom. Phantom was a styrofoam rectangular thoracic phantom (18 × 18 × 24 cm), which was filled with water containing a uniform concentration of radionuclide. The cardiac phantom had a myocardial volume of 130 ml that surrounded a central cavity. The lung tumor phantom had a volume of 10 ml. From our phantom studies, the scatter correction coefficient, α, was 1.07, whereas the crosstalk correction coefficient, β, was 0.14 (*3*). The corrected counts in the 71-keV window for the ^{201}Tl image (a) and in the 140-keV window for the ^{99m}Tc image (b) were as follows: $a = A - \alpha C$ and $b = B - \beta a$, where A represents the raw counts in the 71-keV window, B represents the raw counts in the 140-keV window and C represents the raw counts in the 90-keV window. No direct extrapolation can be made from the results of this phantom study to clinical situations for several reasons. The cardiac and lung tumor phantom was stationary, whereas the lungs and heart are moving in the clinical situation. Sequential radioisotope studies are preferable. Further investigation and clinical validation of the dual-isotope method were performed. However, dual-isotope imaging in one scan would reduce the potential for errors induced by image misalignment and decrease patient discomfort from longer procedures.

Data Analysis

SPECT images were compared with chest radiographs and CT, and accumulation in lung tumors was evaluated by two radiologists. For all patients studied, the coronal slices were evaluated first, followed by the transverse and sagittal views. Semiquantitative analysis of the abnormal uptake of the two radiopharmaceuticals was performed by drawing identical regions of interest (ROIs) over the tumor uptake and contralateral lung tissue areas on one coronal section that demonstrated the lesion most clearly and was carefully selected on both early and delayed images. The mean ROI values (total counts/total pixels) were measured, and the tumor-to-normal (T/N) ratios were obtained. We called the T/N ratio of early image the early ratio and the T/N ratio of delayed image the delayed ratio. To semiquantitatively evaluate the degree of retention in the lesion, the retention index was calculated using the following formula: (delayed ratio − early ratio) × 100/early ratio. The value of the T/N ratio and retention index were expressed as the mean ± s.d. To test for differences between these parameters, the Student's t-test was used. Results were considered significant when $p < 0.05$.

RESULTS

Table 1 presents the clinical findings and semiquantitative values for all patients examined. The early ratio, delayed ratio and retention index are shown in detail in Tables 2 and 3. Both early and delayed ratios using ^{99m}Tc-MIBI SPECT in CR (Fig. 1) and PR groups were significantly higher ($p < 0.05$) than those in the NC group (Fig. 2). There were no significant differences in either ratio among the three groups using ^{201}Tl-chloride SPECT images. There were no significant differences in the retention index among the three groups using both ^{201}Tl-chloride and ^{99m}Tc-MIBI.

TABLE 1
Clinical Findings

Patient no.	Stage	^{201}Tl E	^{201}Tl D	MIBI E	MIBI D	Response
1	III A	2.7	2.9	2.5	2.6	CR
2	IV	4.5	4.6	3.0	4.3	CR
3	III B	3.3	4.5	2.5	2.2	PR
4	III B	2.6	4.6	1.3	1.7	NC
5	III A	2.3	2.4	2.5	3.0	CR
6	IV	5.1	4.4	4.2	3.4	PR
7	I	2.5	3.3	1.8	2.0	CR
8	III B	4.3	4.1	3.9	4.0	CR
9	IV	5.0	5.0	2.6	1.9	NC
10	IV	2.2	3.0	2.5	2.5	PR
11	IV	2.6	3.9	1.5	1.8	NC
12	IV	4.0	4.0	3.3	3.1	PR
13	III A	4.0	4.1	3.2	3.4	PR
14	III A	2.6	2.7	2.2	2.3	PR
15	III A	3.5	4.0	1.6	1.0	NC
16	IV	1.8	1.6	1.0	1.0	NC
17	IV	2.7	2.4	1.6	1.3	NC
18	IV	2.0	2.4	1.7	2.0	PR
19	IV	4.6	4.8	4.3	4.6	CR

E = early ratio; D = delayed ratio; CR = complete remission; PR = partial remission; NC = no change.

DISCUSSION

Various radiopharmaceutical agents have been used in lung cancer assessment, commonly ^{67}Ga and ^{201}Tl (*1,2*). The mech-

TABLE 2
Semiquantitative Analysis of Technetium-99m-Sestamibi (MIBI)

Follow-up group	n	MIBI SPECT E	MIBI SPECT D	RI
CR	6	3.00 ± 0.94*	3.42 ± 1.04*	14.66 ± 15.38
PR	7	2.80 ± 0.83*	2.70 ± 0.59*	−1.24 ± 12.27
NC	6	1.60 ± 0.54	1.45 ± 0.40	−5.40 ± 27.04

*$p < 0.05$ compared to NC (by Student's t test).
E = early ratio; D = delayed ratio; RI = retention index; CR = complete remission; PR = partial remission; NC = no change.

TABLE 3
Semiquantitative Analysis of Thallium-201-Chloride

Follow-up group	n	^{201}Tl SPECT E	^{201}Tl SPECT D	RI
CR	6	3.48 ± 1.09	3.68 ± 0.97	7.61 ± 12.61
PR	7	3.31 ± 1.13	3.59 ± 0.86	12.19 ± 19.21
NC	6	3.03 ± 1.10	3.58 ± 1.32	19.83 ± 36.08

E = early ratio; D = delayed ratio; RI = retention index; CR = complete remission; PR = partial remission; NC = no change.

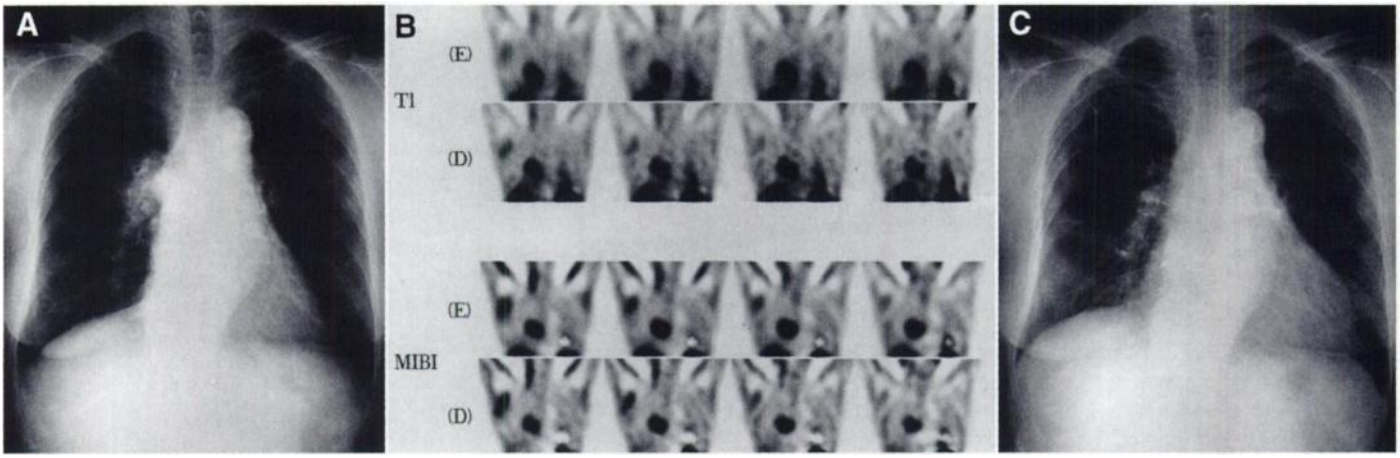

FIGURE 1. Radiologic findings in Patient 1. (A) Chest x-ray showing an abnormal shadow at the right hilum before chemotherapy. (B) Coronal SPECT images of both ^{201}Tl-chloride and ^{99m}Tc-MIBI SPECT demonstrate an abnormal accumulation corresponding to the lesion. E = early image; D = delayed image. (C) Chest x-ray showing no tumor after chemotherapy.

anism of ^{201}Tl-chloride uptake in the cell has been reported to be related to the sodium–potassium adenosine triphosphate (ATP) pump system (*4,5*). Thallium-201-chloride behaves like potassium in the metabolic cycle for the release of energy, and its uptake is blocked by ouabain (*6*).

Since the late 1980s, there has been an increasing number of studies describing ^{99m}Tc-MIBI uptake in several tumors, including lung tumors (*7–13*). The mechanism of ^{99m}Tc-MIBI uptake is different from that of ^{201}Tl-chloride. The uptake of ^{99m}Tc-MIBI is not blocked by ouabain and is not related to the ATP system. It has been shown that ^{99m}Tc-MIBI is attached to a low molecular weight protein in the lysosomes. The cationic charge and lipophilicity of ^{99m}Tc-MIBI, the mitochondrial and plasma membrane potentials of the tumor cell and the cellular mitochondrial content may play a significant role in the tumor uptake of this agent (*14*). The uptake may be caused by an indirect mechanism such as increased tumor blood flow and capillary permeability. Recent investigations suggest the hypothesis that ^{99m}Tc-MIBI may interact with P-glycoprotein (Pgp), a 170-kDa cytoplasmic membrane protein encoded by the *MDR1* gene, which displays decreased cytotoxic drug (such as anthracyclins, *Vinca* alkaloids, epipodophyllotoxin, colchicine and actinomycin D) accumulation (*15–20*). Multidrug resistance results from the action of Pgp as an energy-dependent drug efflux pump. General methods of detecting *MDR1* expression in tissues include assessing DNA amplification, measurement of mRNA and quantitation of Pgp. The data reported by Piwnica-Worms et al. (*20*) indicate that ^{99m}Tc-MIBI is a transport substrate recognized by Pgp, and thallium is not recognized as a substrate by Pgp. Pgp overexpression has been associated with clinical evidence of drug resistance and treatment failure (*21*). It has been suggested that determination of Pgp levels in patients at diagnosis or relapse may have a major role in the design of future treatment protocols. Moretti et al. (*22*) reported a case of small cell lung cancer demonstrating uptake on ^{111}In-octreotide scintigraphy but an absence of radionuclide uptake using ^{99m}Tc-MIBI. The patient failed to respond to chemotherapy and eventually died. The authors suggested the presence of multidrug resistance (MDR)-mediated Pgp in the tumor, which avoids ^{99m}Tc-MIBI concentration by acting as an efflux pump, and ^{99m}Tc-MIBI may prove useful for functionally characterizing Pgp expression and MDR in human tumors in vivo.

In this study, there was no significant correlation between the T/N ratio using ^{201}Tl-chloride SPECT and the chemotherapeutic response of tumor. There was a tendency for the retention index in the NC group to be higher than that in the CR and PR groups, but there were no significant differences among the three groups. On the other hand, early and delayed ratios using ^{99m}Tc-MIBI SPECT in CR and PR groups were significantly

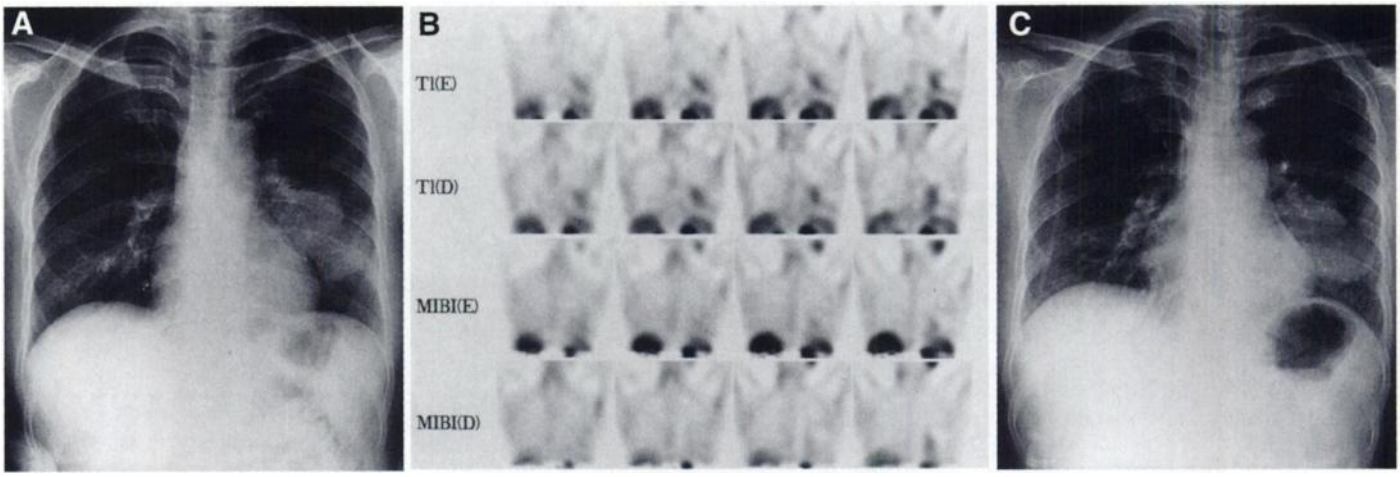

FIGURE 2. Radiologic findings in Patient 15. (A) Chest x-ray showing a large mass shadow at the lower part of the left lung. (B) Early and delayed images of ^{201}Tl-chloride SPECT demonstrate an abnormal accumulation corresponding to the lesion. Technetium-99m-MIBI SPECT did not demonstrate an abnormal accumulation corresponding to the lesion in either early or delayed images. E = early image; D = delayed image. (C) Chest x-ray after chemotherapy showing no decrease in the size of tumor.

higher than those in the NC group. There was a tendency for the retention index in the NC group to be lower than those in the CR and PR groups, but there was no significant difference among the groups. The use of ^{99m}Tc-MIBI is possibly applicable to the prediction of chemotherapeutic efficacy, which is difficult using morphologic imaging techniques such as CT and MRI. However, we cannot conclude this with certainty because quantification of Pgp molecules with other conventional methods was not performed. To determine therapeutically significant Pgp density, further clinical studies correlating ^{99m}Tc-MIBI imaging with quantitative mRNA assays as well as clinical outcome need to be performed. Technetium-99m-MIBI uptake in a tumor dose does not necessarily indicate that a cancer is sensitive to drugs associated with MDR, because there are many other mechanisms for resistance to multiple drugs, such as changes in the activity of glutathione S-transferase, alterations in topoisomerase II (*23*) and expression of MDR-associated protein (190 kDa) (*24*). Hendrikse et al. (*25*) reported that ^{99m}Tc-MIBI is a substrate for the multidrug resistance-associated protein, an alternative transporter discovered by Cole et al. (*26*). An extensive study by Lai et al. (*27*) revealed only low levels of *MDR1* mRNA expression in patients with small cell lung cancer. We did not, however, have sufficient numbers of patients with small cell lung cancer to arrive at a statistically meaningful conclusion. Further work in this area, including the relationship between ^{99m}Tc-MIBI and multidrug resistance, needs to be conducted.

CONCLUSION

Technetium-99m-MIBI SPECT may be more effective than ^{201}Tl-chloride SPECT for evaluating the response to chemotherapy in patients with small cell lung cancer. However, the accuracy of these scintigraphic methods is yet to be verified with additional techniques at the molecular level.

REFERENCES

1. Matsuno S, Tanabe M, Kawasaki Y, et al. Effectiveness of planar image and single-photon emission computed tomography of thallium-201 compared with gallium-67 in patients with primary lung cancer. *Eur J Nucl Med* 1992;19:86–95.
2. Tonami N, Shuke N, Yokoyama K, et al. Thallium-201 single photon emission computed tomography in the evaluation of suspected lung cancer. *J Nucl Med* 1989;30:997–1004.
3. Yamamoto Y, Kusuhara T, Kumazawa Y, et al. The effect of scattering in simultaneous acquisitions of ^{99m}Tc and ^{201}Tl–a fundamental study through phantom experiments. *Radioisotopes* 1996;45:369–374.
4. Kishida T. Mechanism of thallium-201 accumulation to thyroid gland: clinical usefulness of dynamic study in thallium-201 chloride scintigraphy for differential diagnosis of thyroid nodules. *Kagu Igaku* 1987;24:991–1004.
5. Ito Y, Muranaka A, Harada T, Matsudo A, Yokobayashi T, Terashima H. Experimental study on tumor affinity of ^{201}Tl-chloride. *Eur J Nucl Med* 1978;3:81–86.
6. Sehweil AM, McKillop JH, Milroy R, Wilson R, Abdel-Dayem HM, Omar YT. Mechanism of ^{201}Tl uptake in tumours. *Eur J Nucl Med* 1989;15:376–379.
7. Hassan IM, Sahweil A, Constantinides C, et al. Uptake and kinetics of Tc-99m hexakis 2-methoxy isobutyl isonitrile in benign and malignant lesions in the lungs. *Clin Nucl Med* 1989;14:333–340.
8. Actolun C, Bayhan H, Kir M. Clinical experience with ^{99m}Tc MIBI imaging in patients with malignant tumors: preliminary results and comparison with ^{201}Tl. *Clin Nucl Med* 1992;17:171–176.
9. Kao CH, Wang SJ, Lin WY, Hsu CY, Liao SQ, Yeh SH. Differentiation of single solid lesions in the lungs by means of single-photon emission tomography with technetium-99m methoxyisobutylisonitrile. *Eur J Nucl Med* 1993;20:249–254.
10. Desai SP, Yuille DL. Visualization of a recurrent carcinoid tumor and an occult distant metastasis by technetium-99m-sestamibi. *J Nucl Med* 1993;34:1748–1751.
11. Strouse PJ, Wang DC. Incidental detection of bronchogenic carcinoma during ^{99m}Tc sestamibi cardiac imaging. *Clin Nucl Med* 1993;18:448–449.
12. Cancer B, Kitapci M, Erbengi G, Gogus T, Bekdik C. Increased accumulation of ^{99m}TC MIBI in undifferentiated mesenchymal tumor and its metastatic lung lesions. *Clin Nucl Med* 1992;17:144–145.
13. Nishiyama Y, Kawasaki Y, Yamamoto Y, et al. Technetium-99m-MIBI thallium-201 scintigraphy of primary lung cancer. *J Nucl Med* 1997;38:1358–1361.
14. Chiu ML, Kronauge JF, Piwnica-Worms D. Effect of mitochondrial and plasma membrane potentials on accumulation of hexakis (2-methoxyisobutylisonitrile) technetium (I) in cultured mouse fibroblasts. *J Nucl Med* 1990;31:1646–1653.
15. Ballinger JR, Hua HA, Berry BW, Firby P, Boxen I. Technetium-99m-sestamibi as an agent for imaging P-glycoprotein-mediated multi-drug resistance: in vitro and in vivo studies in a rat breast tumour cell line and its doxorubicin-resistant variant. *Nucl Med Commun* 1995;16:253–257.
16. Dimitrakopoulou-Strauss A, Strauss LG, Goldschmidt H, Lorenz WJ, Maier-Borst W, Van Kaick G. Evaluation of tumour metabolism and multidrug resistance in patients with treated malignant lymphomas. *Eur J Nucl Med* 1995;22:434–442.
17. Rao VV, Chiu ML, Kronauge JF, Piwnica-Worms D. Expression of recombinant human multidrug resistance P-glycoprotein in insect cells confers decreased accumulation of technetium-99m-sestamibi. *J Nucl Med* 1994;35:510–515.
18. Komori T, Matsui R, Adachi I, Shimizu T, Sueyoshi K, Narabayashi I. In vitro uptake and release of ^{201}Tl and ^{99m}Tc-MIBI in HeLa cell. *Kaku Igaku* 1995;32:651–658.
19. Ford JM, Hait MN. Pharmacology of drugs that alter multidrug resistance in cancer. *Pharmacol Rev* 1990;42:155–199.
20. Piwnica-Worms D, Chiu ML, Budding J, et al. Functional imaging of multidrug-resistant P-glycoptotein with an organotechnetium complex. *Cancer Res* 1993;53:977–984.
21. Chan HLS, Haddad G, Thorner PS, et al. P-Glycoprotein expression as a predictor of the outcome of therapy for neuroblastoma. *N Engl J Med* 1991;325:1608–1614.
22. Moretti JL, Caglar M, Boaziz C, Caillat-Vigneron N, Morere JF. Sequential functional imaging with technetium-99m hexakis-2-methoxyisobutylisonitrile and indium-111 octreotide: can we predict the response to chemotherapy in small cell lung cancer? *Eur J Nucl Med* 1995;22:177–180.
23. Morrow CS, Cowan KH. Mechanisms of antineoplastic drug resistance. In: De Vita V, Hellman S, Rosenberg SA, eds. *Cancer: principles and practice of oncology.* Philadelphia: Lippincott; 1993:340–348.
24. Deeley RG, Grant CE, Almquist KC, et al. Multidrug resistance mediated by the 190 kDa MRP: a novel member of the ATP-binding cassette transporter superfamily. *Proc Am Assoc Cancer Res* 1994;35:698–699.
25. Hendrikse NH, Franssen EJF, van der Graaf WTA, Meijer C, de Vries EGE. Reduced ^{99m}Tc-sestamibi accumulation in Pgp-positive and MRP-positive cell lines [Abstract]. *Proc Am Assoc Cancer Res* 1995;36:358.
26. Cole SPC, Bhardwaj G, Gerlach JH, et al. Overexpression of a transporter gene in a multidrug-resistant human cancer cell line. *Science* 1992;258:1650–1654.
27. Lai SL, Goldstein LJ, Gottesman MM, et al. *MDR1* gene expression in lung cancer. *J Natl Cancer Inst* 1989;81:1144–1150.